Received May 7, 2018, accepted June 4, 2018, date of publication June 13, 2018, date of current version July 6, 2018.

Digital Object Identifier 10.1109/ACCESS.2018.2845411

The Design Method of the Active Negative Group Delay Circuits Based on a Microwave Amplifier and an RL-Series Network

FAYU WAN[1], (Member, IEEE), NINGDONG LI[1], BLAISE RAVELO[2], (Member, IEEE), QIZHENG JI[3], BINHONG LI[4], AND JUNXIANG GE[1]

[1]Nanjing University of Information Science and Technology, Nanjing 210044, China
[2]Normandy University, UNIROUEN, ESIGELEC, IRSEEM,76801 Rouen, France
[3]Beijing Orient Institute of Measurement and Test, China Academy of Space Technology, Beijing 100080, China
[4]Key Laboratory of Silicon Device Technology, Chinese Academy of Sciences, Beijing 100864, China

Corresponding author: Qizheng Ji (jiqizheng790308@sina.com)

This work was supported in part by NSFC under Grant 61601233 and Grant 61750110535, in part by the Defense Research Foundation under Grant 6140209050116ZK53001, in part by NSF of Jiangsu under Grant BK20150918, in part by the Jiangsu Innovation and Enterprise Group Talents Plan 2015 under Grant SRCB201526, and in part by PAPD.

ABSTRACT This paper addresses a circuit theory regarding the negative group delay (NGD) principle. The methodology for characterizing this unfamiliar NGD function is described. The basic NGD topology under study is typically an active cell composed of an RF low-noise amplifier (LNA) and an RL-series passive network. It acts as a low-pass NGD topology. The family of the bandpass NGD cell is identified from the low-pass to the bandpass transform. The NGD circuit theory under study is essentially built with the S-parameter approach. The main characteristics of the proposed NGD topology and properties of the NGD level, cut-off frequencies or bandwidth, central frequency, and figure-of-merit are established. The NGD cell is synthesized using the LNA S-parameter model. A method for designing the low- and bandpass NGD cells as a function of the specified NGD values is presented. The NGD cell parameter calculations as functions of the expected NGD level, insertion loss, and reflection coefficient are introduced. Proof-of-concept NGDs are synthesized, designed, simulated, and fabricated to understand and validate the proposed NGD low-pass and bandpass functions. As expected, low-pass and bandpass NGD aspects are obtained. The low-pass NGD circuits present an NGD level of approximately -5 ns over the bandwidth fc $= 25$ MHz. Next, bandpass NGD circuits were synthesized to operate at approximately 0.5 GHz over the bandwidth Δf $= 50$ MHz with an NGD level of approximately -10 ns. The measured results of the low-pass and bandpass NGD are in good agreement with the theoretical prediction obtained with simple lumped circuits. Different applications of the unfamiliar NGD function are described.

INDEX TERMS Negative group delay (NGD) principle, low noise amplifier (LNA), RL-passive network, NGD characterization, synthesis method, microwave circuit theory, low-pass NGD circuit, band-pass NGD circuit.

I. INTRODUCTION

Since the 1990s, the negative group delay (NGD) phenomenon has been investigated theoretically and experimentally using low-frequency and RF/microwave electronic circuits [1]–[6]. In this period, the intriguing phenomenon was independently studied in two different manners. In one manner, the NGD function was synthesized using passive microwave circuits [1]–[2]. In the other manner, the NGD active circuits operating at very low frequencies below megahertz were identified [3]–[5]; these low frequency NGD circuits, which are constituted by classical components of R, L, C and an operational amplifier [3], were inspired by an atomic medium at optical wavelengths [6]. The NGD effect was initially observed in the propagation media presenting anomalous dispersion [7], [8]. It was noted that the NGD effect is generated in an abnormal media frequency band presenting a negative refractive group index $n_g(\omega)$ as a function of the angular frequency ω or the wavelength [9]. Because of the dispersion, this refractive group index can be negative at certain wavelengths. Moreover, the group

velocity $v_g(\omega)$ can also be negative, as analytically illustrated by

$$v_g(\omega) = \frac{c}{n_g(\omega)} \tag{1}$$

where c is the speed of light in a vacuum. In other words, when using a propagation medium with geometrical length d, the group delay, defined as

$$\tau_g(\omega) = \frac{d}{v_g(\omega)} \tag{2}$$

can also be negative. Because of the wave reshaping or the combination of the constructive and destructive interferences at the edge of the abnormal dispersive passive medium, the NGD phenomenon is systematically accompanied by significant losses at microwave wavelengths [10], [11]. The NGD phenomenon was classified among the abnormal physical phenomena as the superluminal signal propagating in a medium with anomalous dispersion [7]–[12]. It was concluded from various experimental results that the NGD phenomenon introduces the possibility to generate an output signal with wave fronts propagating in advance of its input under certain conditions [13]–[15]. Opposite to the classical ordinary structure, in the case of NGD media, the time delay can be assumed as negative [13]–[15]. Note that this NGD effect does not violate the causality principle [4], [5].

The first tentative application of the NGD function for signal delay cancellation was proposed in 2002 [16]. However, because of the NGD bandwidth limitations to some hundred kilohertz, the possibility of applications was technically restrained and was not successful. This limitation explains the main interest in developing NGD circuits capable of operating at RF and higher frequencies. Microwave NGD passive circuits based on resonant filter topologies presenting absorption phenomena have been identified [17], [18]. As a result, the applications of NGD passive circuits remained limited before the middle 2000s. During the same period, other NGD circuits, inspired by left-handed metamaterial structures, were also identified [19]–[21]. With metamaterial-based NGD circuits, the time-advance aspect was experimentally studied in the time-domain at microwave wavelengths [21]. More recently, NGD-distributed microwave circuits have been developed with coupling effects [22]–[24]. However, the passive NGD circuits are systematically absorbing or exhibit outstanding reflections that limit the application possibilities.

To overcome this limitation, active microwave topologies with NGD effect were developed [25]–[31]. First, a design method for enhancing the feedforward amplifier with NGD function was proposed. However, the circuit is dedicated only to the feedforward configuration application and cannot be generalized as an elementary NGD cell. Then, simpler topologies based on the RF/microwave transistors have been developed [27]–[31]. It was emphasized in [32] that the NGD values are a limited function of the topology parameters. A methodology to identify elementary field effect transistor (FET)-based NGD topologies has been introduced [34]. It was also emphasized that the intriguing NGD function presents similar behaviors to those of the classical NGD filter [30]. The electronic circuit NGD bandwidth can be defined as the frequency bands where the group delay is negative. Different types of NGD aspects, such as low-pass and band-pass NGD circuits, have been categorized [30]. Note that because of the transistor access-matching difficulties, the complexity of the biasing networks and the output voltage sign inversion compared to the input is found with certain NGD topologies, as proposed in [24]. In other words, somehow, the use of transistors is increasingly sophisticated. To avoid the complexity of a bias network and the issues related to the matching level, the replacement of the transistor by an integrated low noise amplifier (LNA) was introduced in [34] and [35] for the base band applications. The other reason that the LNA is used to replace transistor is that the first stage of the circuit is a high-loss structure. Its noise characteristics may not be good. The LNA helps to reduce the noise figure of the whole circuit. Despite this trend of the NGD theory democratization and exploration of applications, various methods of exploring the NGD concept are still required for further understanding through academic and industrial perspectives. An alternative method to design NGD active RF/microwave circuits involves replacing the FET with an LNA. This alternative can be a solution for access matching, stability and bias circuit simplification. This aspect can be significantly important for the design simplicity.

In the present paper, an easy-to-understand circuit theory of the NGD principle with an LNA-based cell is introduced. To build the theory, the LNA component is modeled by the touchstone S-parameter. This basic theoretical approach contains the basic principle and analysis that allows the NGD concept to be familiar to electrical engineering students, researchers and industries. A simple low-pass topology consisting of an RL series passive network is developed. It acts as a first-order circuit. The cell can be investigated similarly for any electrical familiar function. The generality regarding the basic topology will be introduced in Section 2. The NGD analysis is focused on the family of shunt impedance type cells. Section 3 analytically develops the NGD characterization. The microwave circuit theory under study is essentially focused on the basic NGD properties and synthesis methodology. Next, by considering the familiarly known low-pass to band-pass circuit transform in filter theory [30], the associated band-pass NGD cell is investigated. The proposed NGD principle is verified with simulations and experimental results in Section 4. Simulation validations of the LNA-based lumped circuits will be described. Section 5 is the conclusion.

II. THE GENERAL ACTIVE CIRCUIT TOPOLOGY UNDER STUDY

A description of the general topology under study is provided in this section. The proposed circuit theory is essentially built

with an S-parameter modeling approach. The NGD principle is introduced with the analytical characterization.

A. BASIC TOPOLOGY

The present subsection generally describes the elementary active microwave circuit topology to be investigated. As noted in [34] and [35], the basic topology consists of an LNA associated with a simple two-port passive network. The simplest passive network of parallel impedance, denoted Z_p, is considered. Note that the analytical calculation will be developed with the LNA S-parameter model defined by

$$[S_{LNA}] = \begin{bmatrix} r & 0 \\ t & r \end{bmatrix}, \tag{3}$$

with the real variables r and t (which are the LNA access reflection coefficient and the insertion gain, respectively) assumed to be independent of frequency in the operating frequency band. The aim of the active circuit is to compensate for the NGD circuit loss. This compensation is very important for the time domain demonstration to clearly show the feasibility of the time advance aspect. This aspect can be visualized both with time domain simulations and time-domain measurements.

B. SHUNT IMPEDANCE-BASED TOPOLOGIES UNDER STUDY

The shunt impedance-based active cells investigated in the present paper are introduced in Fig. 1. The three considered configurations depend on the position of the passive network placed upstream or downstream of the LNA. Note that Z_0 represents the reference impedance equal to 50 Ω.

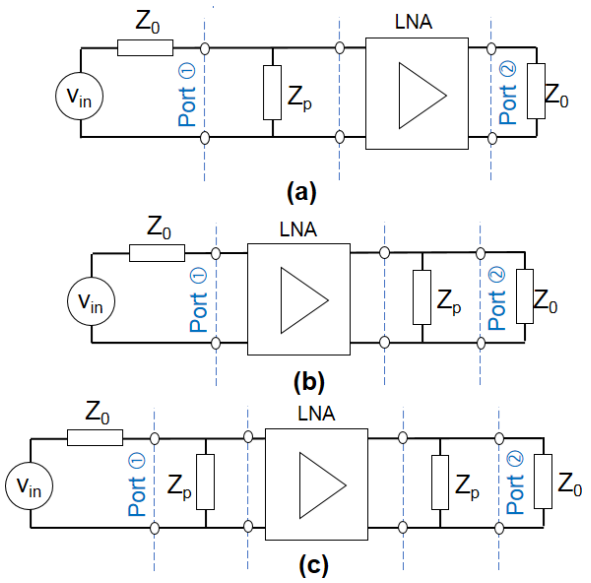

FIGURE 1. (a) Parallel impedance and LNA in cascade. (b) LNA and parallel impedance in cascade. (c) Active cell with double shunt impedance.

Acting as a cascaded circuit configuration, the analytical calculations of the S-parameter can be obtained from the total circuit transfer matrix. According to the circuit and system theory, the total transfer matrix is equal to the non-commutative product of the cascaded constituting cells that are represented by the impedance and the LNA in the present case. By applying the S-parameter theory, the following expressions have been established:

-For the parallel impedance-based cell with LNA inserted downstream, as presented in Fig. 1(a):

$$[S_{p-LNA}(j\omega)] = \begin{bmatrix} \dfrac{2rZ_p - (1+r)R_0}{2Z_p + (1+r)R_0} & 0 \\ \dfrac{2tZ_p}{2Z_p + (1+r)R_0} & r \end{bmatrix} \tag{4}$$

-For the parallel impedance-based cell with LNA inserted upstream, as presented in Fig. 1(b):

$$\begin{aligned}[S_{LNA-p}(j\omega)] &= \begin{bmatrix} r & 0 \\ S_{p-LNA_{21}}(j\omega) & S_{p-LNA_{11}}(j\omega) \end{bmatrix} \\ &= \begin{bmatrix} r & 0 \\ \dfrac{2tZ_p}{2Z_p+(1+r)R_0} & \dfrac{2rZ_p - (1+r)R_0}{2Z_p + (1+r)R_0} \end{bmatrix} \end{aligned} \tag{5}$$

-For the parallel impedance-based cell with LNA inserted both up- and down-stream, as presented in Fig. 1(c):

$$\begin{aligned}&[S_{p-LNA-p}(j\omega)] \\ &= \begin{bmatrix} S_{p-LNA_{11}}(j\omega) & 0 \\ \dfrac{S^2_{p-LNA_{21}}(j\omega)}{t} & S_{p-LNA_{11}}(j\omega) \end{bmatrix} \\ &= \begin{bmatrix} \dfrac{2rZ_p - (1+r)R_0}{2Z_p + (1+r)R_0} & 0 \\ \dfrac{4Z_p^2 t}{[2Z_p + (1+r)R_0]^2} & \dfrac{2rZ_p - (1+r)R_0}{2Z_p + (1+r)R_0} \end{bmatrix} \end{aligned} \tag{6}$$

The proposed topology isolation parameters $S_{12} = 0$ because of the LNA unilaterality.

C. PRINCIPLE OF NGD ANALYSIS

By denoting $j\omega$ as the circuit angular frequency variable, according to the circuit and system theory, recall that the group delay is defined by

$$\tau(\omega) = -\frac{\partial\varphi(\omega)}{\partial\omega} \tag{7}$$

where

$$\varphi(\omega) = \angle S_{21}(j\omega) \tag{8}$$

is the transmission phase in radians. This last expression shows that our impedance cannot be a frequency-independent component, such as a simple resistor. In other words, to generate non-zero group delay, a reactive element-based circuit is necessary. As a result, we examined different configurations of first-order RL-series parallel networks. Based on the RF/microwave engineering, the main circuit parameters are basically the access matching and the insertion loss (for the passive circuits) or the insertion gain (for the active circuits). Those parameters are still under consideration in the

present study. In addition, we are also considering the group delay defined in equation (7). The NGD characterization described in this section is mainly obtained from the analytical expression of the S-parameters and group delay at very low frequencies, when $\omega \approx 0$. The low-pass NGD characteristics can be determined with the following parameters:

The NGD level is analytically defined as $\tau(\omega \approx 0) = \tau(0)$.

The NGD cut-off angular frequency ω_c corresponds to the root of the equation $\tau(\omega_c) = 0$. Both parameters can be integrated in the unified NGD figure-of-merit (FoM), which is defined by

$$FoM_{NGD} = \tau(0) \cdot \omega_c \tag{9}$$

The better the NGD circuit, the higher the FoM is.

D. NGD MICROWAVE CIRCUIT DESIGN METHOD

The microwave circuit theory enabling the design of low-pass and band-pass NGD circuits based on the familiar electronic components R, L and C will be presented in the two next sections. After exploring the existence of the NGD effect with two lumped element-based passive topologies, the possibility of compensating for the loss by inserting an LNA in the cascade with the passive NGD network will be investigated. The theoretical characterization of the obtained active circuit will be described. As will be described, to compensate for the NGD passive circuit loss attenuation $A < 1$, we can simply insert an LNA with gain equal to the following:

$$G = 1/A. \tag{10}$$

At the end of each step, synthesis expressions facilitating the calculation of the NGD circuit parameters as a function of the NGD specifications will be formulated.

III. NGD ANALYSIS OF THE RL-PASSIVE NETWORK-BASED ACTIVE CELL

The analytical identification performed in [29] states that the following is the only configuration for a first-order or low-pass NGD circuit associated with the parallel impedance configuration is an RL-series network:

$$Z_p(j\omega) = R + j\omega L \tag{11}$$

Using the LNA model defined in equation (3), the characterization and synthesis methods will be analytically developed.

A. LOW-PASS CELL WITH LNA

Fig. 2 represents the configurations of the RL-series parallel passive network. These cells are low-pass NGD elementary circuits. According to (4), (5) and (6), these cells generate similar reflection and transmission coefficients. However, only the cell shown in Fig. 2(c) enables the control of both the input and output reflection coefficients. The remainder of this paper is focused on the case of a cell with up- and down-stream RL-network configurations.

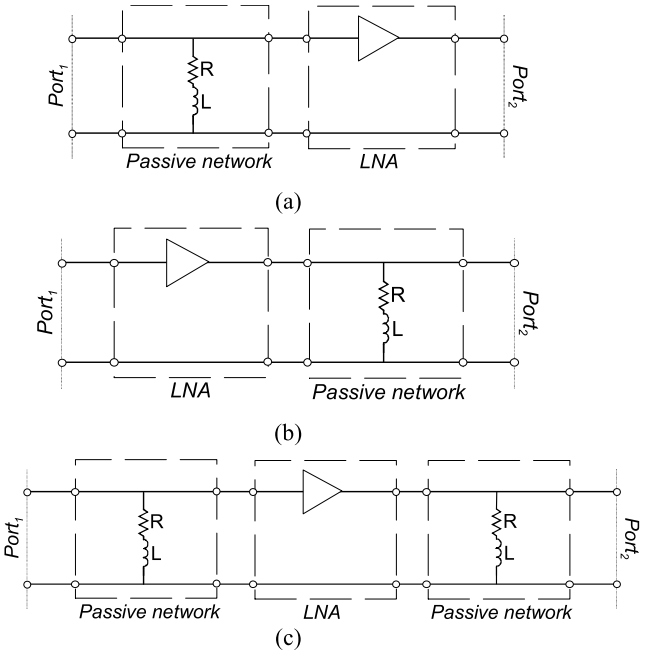

FIGURE 2. LNA-based low-pass NGD cell with an RL-series shunt network (a) upstream, (b) downstream, and (c) up- and down-stream.

1) FREQUENCY-DEPENDENT S-PARAMETER AND GROUP DELAY

The S-parameter model of the cell shown in Fig. 2(c) can be deduced from the general expression established in (6). Substituting Z_p with the expression introduced in (11), the following expression is obtained as a function of the parallel impedance-based cell with LNA parameters (12), as shown at the bottom of the next page.

2) NGD CHARACTERIZATION AND PROPERTIES

At very low frequencies, the S-parameters of the parallel impedance-based circuit become:

$$\left[S_{pl}(0)\right] = \begin{bmatrix} \dfrac{2rR - (1+r)R_0}{2R + (1+r)R_0} & 0 \\ \dfrac{4R^2 t}{[2R + (1+r)R_0]^2} & \dfrac{2rR - (1+r)R_0}{2R + (1+r)R_0} \end{bmatrix} \tag{13}$$

The associated group delay is given by:

$$\tau_{pl}(0) = \frac{-2(1+r)R_0 L}{R\,[2R + (1+r)R_0]} \tag{14}$$

According to the group delay expressed in equation (14), the passive cell introduced in Fig. 2(c) behaves as a low-pass NGD circuit. In addition to the previous characteristics, one of the most important properties of the NGD cell is the NGD cut-off frequency denoted ω_{pc}, which can be assumed as the root of equation $\tau_{pl}(\omega_{pc}) = 0$ and is given by:

$$\omega_{pc} = \frac{\sqrt{2R\,[2R + (1+r)R_0]}}{2L} \tag{15}$$

Based on the above discussion, we can determine the NGD FoM by the following relation:

$$FoM_p = \tau_{pl}(0) \cdot \omega_{pc} = \frac{-2(1+r)R_0}{\sqrt{2R\,[2R+(1+r)R_0]}} \tag{16}$$

It can be underlined that in this case, the NGD FoM is inversely proportional to the resistance R.

3) NGD SYNTHESIS METHOD

The synthesis method consists merely of the calculation of the NGD circuit parameters as a function of the following:

- NGD level τ_0, which is inversely linked to the NGD bandwidth
- Insertion loss or insertion gain
- Reflection coefficients

In other words, we assume that the desired gain g >0 and group delay τ_0, which is assumed to be negative, are known. Analytically, the synthesis formulas are generated from the following equations:

$$\begin{cases} S_{pl_{21}}(0) = g \\ \tau_{pl}(0) = \tau_0 \end{cases} \tag{17}$$

As argued previously, the synthesis formulas are merely the roots of previous equations (13) and (14). For the parallel impedance-based cell, after calculations, we obtain the expressions of R and L associated with the RL-series cell. The synthesis relations for this low-pass NGD cell are as follows:

$$R = \frac{\sqrt{g}(1+r)}{2(\sqrt{t}-\sqrt{g})}R_0 \tag{18}$$

$$L = \tau_0 R\left[\frac{1}{2} + \frac{R}{(1+r)R_0}\right] \tag{19}$$

It can be understood from equation (18) that the synthesized resistance is realistic only if the existence condition $g < t$ is respected. Based on these synthesis formulas, the reflection coefficient can be rewritten as a function of the desired gain as follows:

$$\left|S_{sl_{11}}(0)\right| = \left|1-(1+r)\sqrt{\frac{g}{t}}\right| \tag{20}$$

Note that the resistance synthesis relation can also be extracted from the desired access matching $S_{11}(0) = m$.

B. BAND-PASS NGD ELEMENTARY CELLS

Similar to the filter theory, the band-pass NGD cells can easily be synthesized from the low-pass ones via the low-pass to band-pass transform [28]. The present subsection is focused on the NGD characteristics of the band-pass NGD cells associated with the previous cells. In this case, to synthesize the associated band-pass NGD cell, we simply need to replace the inductance L with an LC-series network. The associated capacitor can be calculated from the inductance and the expected NGD center angular frequency, which is denoted as ω_0. Therefore, we have the capacitor synthesis formula:

$$C_p = \frac{1}{\omega_0^2 L} \tag{21}$$

Fig. 3 represents the configuration of the RLC-shunt network-based band-pass NGD elementary cells corresponding to the low-pass NGD cells shown in Fig. 2.

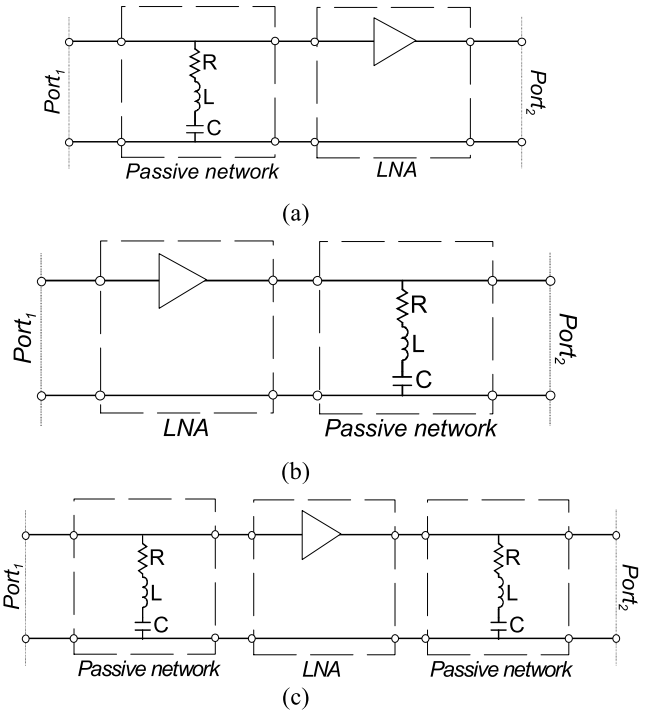

FIGURE 3. LNA-based band-pass NGD cell with RLC-series shunt network (a) upstream, (b) upstream, and (c) up- and down-stream.

1) NGD CHARACTERIZATION AND PROPERTIES

By applying the S-parameter theory, we obtain the transmission gain, reflection coefficient and group delay. For NGD band-pass active cells, the associated S-parameters at the center frequency are expressed as follows:

$$\left[S_{pb}(j\omega_0)\right] = \left[S_{pl}(0)\right] \tag{22}$$

$$\left[S_{pl}(j\omega)\right] = \begin{bmatrix} \dfrac{2r(R+j\omega L)-(1+r)R_0}{2(R+j\omega L)+(1+r)R_0} & 0 \\ \dfrac{4t(R+j\omega L)^2}{[2(R+j\omega L)+(1+r)R_0]^2} & \dfrac{2r(R+j\omega L)-(1+r)R_0}{2(R+j\omega L)+(1+r)R_0} \end{bmatrix} \tag{12}$$

The associated group delay is given by:

$$\tau_{pb}(\omega_0) = \tau_{pl}(0) = \frac{-4(1+r)R_0L}{R\,[2R+(1+r)R_0]} \tag{23}$$

2) NGD SYNTHESIS METHOD

Similar to the previous paragraph, the synthesis formulas of the active cell can be obtained from equations (22) and (23). For the considered parallel impedance-based cell, the expressions of Rand L associated with the RL-series cell can be determined analytically. The synthesis relations for this band-pass NGD cell can be expressed by functions of the resistance and inductance suggested in equations (18) and (19):

$$R_b = R \tag{24}$$

$$L_b = L/2. \tag{25}$$

IV. SIMULATION AND MEASUREMENT RESULTS

The present section is focused on the illustrative feasibility of the low-pass and band-pass NGD functions with the previously introduced topologies. The proof-of-concept (POC) circuits are constituted by a low-pass NGD circuit based on the RL-series parallel network with its band-pass circuit family with an RLC-parallel network.

A. DESCRIPTION OF THE POC CIRCUIT PARAMETERS

The proposed POC circuits were designed with the surface mounted monolithic LNA LEE-9+ from mini-circuits. During the calculation, we assume that the LNA is specified by the transmission gain $t = 8.5$ dB and input/output reflection coefficient average value $r = -22$ dB. The considered NGD circuits were biased with $V_0 = 5V_{DC}$ power supply. In addition to the NGD circuit RF part, the bias network includes self-inductance $L = 75$ nH and $C_p = 100$ pF. The DC blocking capacitors are $C = 100$ pF. As can be understood in the previous theory of Section 3, the NGD circuit under study can be designed similarly to classical and familiar electronic RF and microwave circuits. The POC-modeled computed results are compared with simulations run in the ADS®environment of the electronic circuit designer and simulator. The proposed S-parameter simulations were performed from DC to 1 GHz. Comparisons of the S-parameter between the circuits integrating the ideal LNA model (defined in equation (3)) and touchstone S-parameter model provided by the manufacturer are presented. The obtained simulation results will be explored in the next paragraphs.

B. SYNTHESIS APPROACH

Table 1 summarizes the synthesized parameter of the shunt impedance-based low-pass cell introduced in Fig. 2(c) and the associated band-pass cell introduced in Fig. 3(c). The band-pass circuit was synthesized to operate at the center frequency $f_0 = 0.5$ GHz.

C. LOW-PASS NGD CELL VALIDATIONS

The synthesis of the proposed low-pass NGD circuit based on the shunt impedance-type circuit shown in Fig. 2(c) is targeted to the specifications g =0 dB and $\tau(0) = -5$ ns. Fig. 4 represents the comparison between the simulated and measured S-parameters obtained from the shunt impedance-based low-pass NGD circuit configured in Fig. 2(c). The ideal and real model-based LNA simulations are very well-correlated. The transmission gain shown in Fig. 4(b) is higher than 0 dB, with flatness of approximately 2.5 dB from DC to 25 MHz. The reflection coefficients exposed in Figs. 4(a) and 4(c) are slightly better than 10 dB.

TABLE 1. Synthesized shunt-based NGD circuit parameters given the expected transmission gain g and group delay $\tau 0 < 0$.

g	τ_0	R	L	C (for the band-pass circuit)
0 dB	-2 ns	42.76 Ω	110 nH	0.92 pF
2 dB		59.47 Ω	190 nH	0.53 pF
0 dB	-5 ns	42.75 Ω	276 nH	0.37 pF
2 dB		59.47 Ω	476 nH	0.21 pF

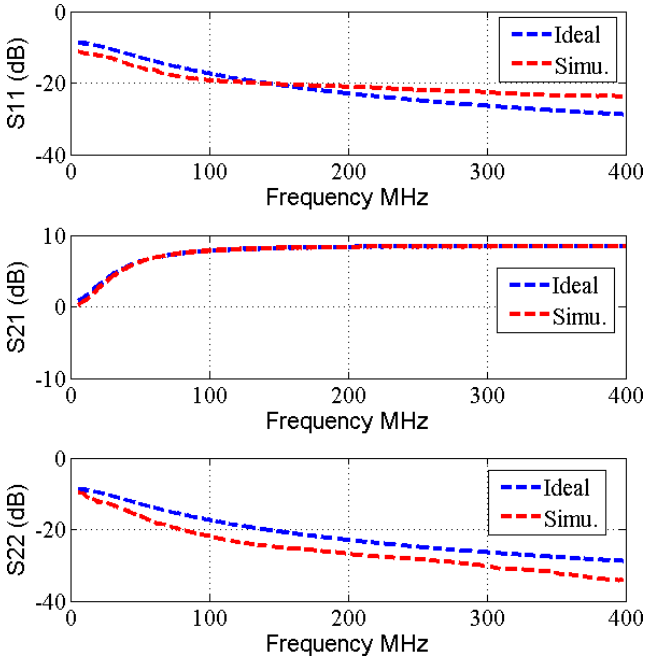

FIGURE 4. S-parameters of low-pass circuits shown in Fig. 2(c).

Fig. 5 displays the simulated group delays from the circuit shown in Fig. 2(c). Despite the discrepancies and parasitic effects of the real LNA-based group delay, a good correlation between the ideal and real LNA based circuits is confirmed. The low-pass NGD function is emphasized by the occurrence of NGD at very low frequencies up to the cut-off frequency of about $f_c = 25$ MHz and positive group delay when the frequency is higher than fc. As expected, low-pass NGD level of approximately -5 ns is obtained. The NGD bandwidth is realized from DC to approximately 25MHz.

D. BAND-PASS NGD CELL VALIDATIONS

The synthesis of the proposed band-pass NGD circuit based on the shunt impedance-type circuit shown in Fig. 3(c) is

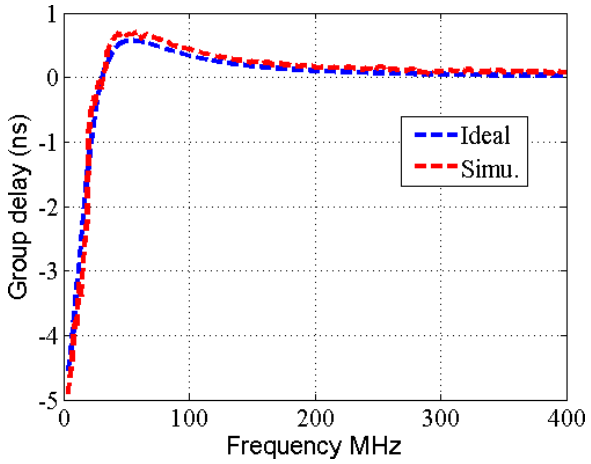

FIGURE 5. Group delays of low-pass circuits shown in Fig. 2(c).

targeted to the specifications $g = 0$ dB and $\tau(f_0) = -10$ ns. Fig. 6 introduces comparisons between the ideal and real LNA-based NGD circuit S-parameters from the circuit shown in Fig. 3(c). As expected, transmission gain above 0 dB is realized in addition to the reflection coefficient better than 10 dB.

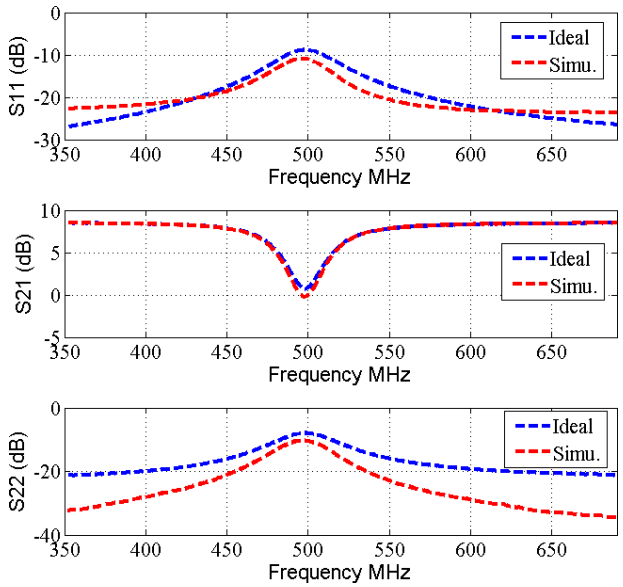

FIGURE 6. S-parameters of band-pass NGD circuits shown in Fig. 3(c).

Fig. 7 displays the group delays of the circuit shown in Fig. 3(c). The ideal and real LNA-based NGD circuit simulations are realized. As expected, a typical band-pass NGD behavior centered at $f_0 = 0.5$ GHz is obtained. The NGD bandwidth is equal to $\Delta f = 2f_c$.

E. EXPERIMENTAL VALIDATION RESULTS

Photographs of the fabricated NGD circuits are shown in Fig. 8. The circuits are printed on FR4 epoxy dielectric substrate. The substrate presents thickness $h = 1.6$ mm,

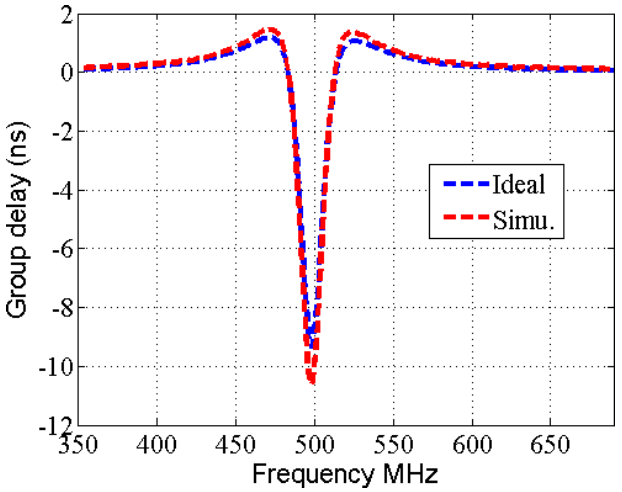

FIGURE 7. Group delays of band-pass NGD circuits shown in Fig. 3(c).

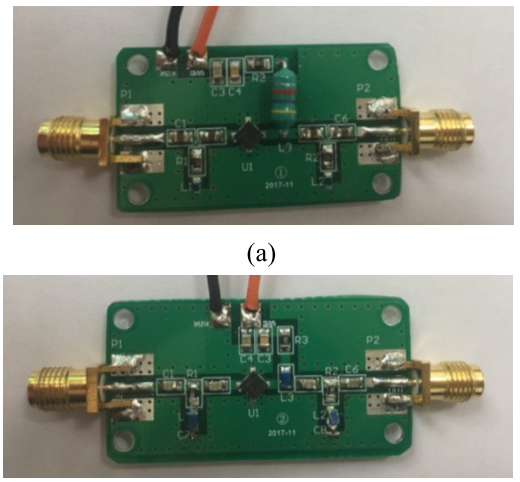

(a) (b)

FIGURE 8. The two fabricated circuits corresponding to (a) low-pass NGD and (b) band-pass NGD.

relative permittivity $\varepsilon_r = 4.4$ and dissipation factor $\tan(\delta) = 0.12$ and $t = 35$ μm thick copper cladding. The metallization conductivity is $\sigma = 58$ MS/m.

The fabricated circuit parameters are addressed in Table 2. The relative tolerances of the resistor and capacitor fabrication are of approximately 5 %. The relative tolerance of the inductor is 10 %. The fabricated circuit prototypes present a physical size of 44.5 mm × 22.5 mm.

TABLE 2. Fabricated circuit parameters.

g	τ_0	R	L	C (for the band-pass circuit)
0 dB	-5 ns	42 Ω	280 nH	0.4 pF

The experimental validation of the proposed low-pass NGD and band-pass NGD is carried out using

S-parameter measurements. The S-parameter measurements are completed using a Vector Network Analyzer (VNA) from Rohde &Schwarz (ZNB 20, frequency band 100 kHz to 20 GHz).

Comparisons between the simulation and measurement results are shown in Fig. 9 and Fig. 10 for the prototypes of the low-pass NGD and band-pass NGD, respectively. As the values of the optimized components may not exist in the real world, the closest nominal value components are chosen. As a result, we observe differences between the simulations and measurements, especially around the center frequency. The measured results correspond to the low-pass NGD, gain $= \{0$ dB$\}$, level $\tau_0 = \{-5$ns$\}$ and the associated band pass NGD. Nevertheless, the measurement frequency responses are considered to be in good agreement with the simulated NGD frequencies, level and bandwidth.

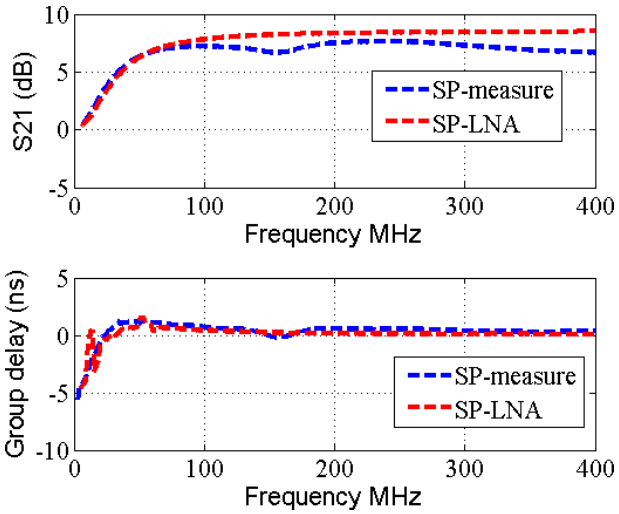

FIGURE 9. S-parameters and Group delay of low-pass NGD circuits.

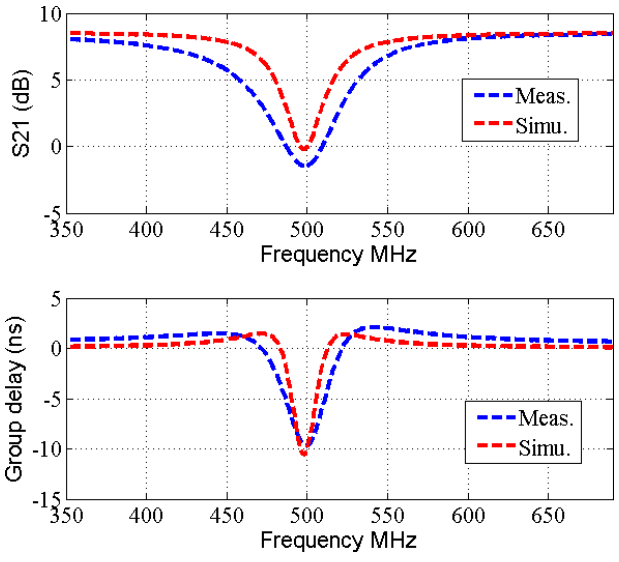

FIGURE 10. S-parameters and Group delay of band-pass NGD circuits.

The obtained results clearly validate the low-pass and band-pass NGD functions under investigation. The relative inaccuracies between the measurements and the simulations are better than 5% (τ_0 is 10% in the band-pass NGD).

The proposed band-pass NGD prototype characteristics are compared with the existing circuits proposed in [20], [23], [29], and [33]. Ass summarized in Table 3, the introduced NGD circuit presents a possibility to generate the most significant NGD absolute value. In addition to the design simplicity, it enables also to avoid the inherent losses.

TABLE 3. Comparison of band pass NGD circuit characteristics with the existing circuit available in [20], [23], [29], [33].

References	f_0 (GHz)	τ_0 (ns)	Δf (MHz)	S_{21} (dB)
[20]	1.30	-4.00	187	-20.00
[23]	1.79	-7.70	35	-8.60
[29]	1.26	-2.2	20	-2.4
[33]	2.14	-1.03	59	-3.8
Proposed one	0.50	-10.00	50	0.00

However, the NGD bandwidth is lower compared to the notably to the passive NGD circuits [20]. This bandwidth can be envisaged with cascaded several NGD cells.

V. CONCLUSION

A microwave circuit theory on the active NGD elementary RF cells was developed. An NGD cell based on the constituting shunt impedance configuration and LNA was explored. The general principle of the NGD analyses was presented. The principle was applied to the NGD circuit family. The analytical principle was established using the S-parameter model. The meaning of low-pass and band-pass NGD functions was illustrated. The main properties of the NGD circuits were developed. The synthesis method enabling the calculation of the NGD circuit parameters was proposed as a function of the specified NGD level and the transmission gain. The theoretical approach was validated with the two types of topologies. Low-pass and band-pass NGD circuits were designed and simulated. As expected, the measurement results and simulation results were found to be in very good correlation with the theoretical prediction. The NGD circuits satisfy all the criteria of RF/microwave circuits.

REFERENCES

[1] S. Lucyszyn, I. D. Robertson, and A. H. Aghvami, "Negative group delay synthesizer," *Electron. Lett.*, vol. 29, no. 9, pp. 798–800, Apr. 1993.
[2] S. Lucyszyn and I. D. Robertson, "Analog reflection topology building blocks for adaptive microwave signal processing applications," *IEEE Trans. Microw. Theory Techn.*, vol. 43, no. 3, pp. 601–611, Mar. 1995.
[3] R. Y. Chiao, E. L. Bolda, J. Bowie, J. Boyce, and M. W. Mitchell, "Superluminality and amplifiers," *Prog. Crystal Growth Characterization Mater.*, vol. 33, nos. 1–3, pp. 319–325, 1996.
[4] M. W. Mitchell and R. Y. Chiao, "Causality and negative group delays in a simple bandpass amplifier," *Amer. J. Phys.*, vol. 66, no. 1, pp. 14–19, 1998.
[5] M. W. Mitchell and R. Y. Chiao, "Negative group delay and 'fronts' in a causal system: An experiment with very low frequency bandpass amplifiers," *Phys. Lett. A*, vol. 230, pp. 133–138, Jun. 1997.
[6] R. Y. Chiao, "Atomic coherence effects which produce superluminal (but causal) propagation of wavepackets," *Quantum Opt., J. Eur. Opt. Soc. B*, vol. 6, no. 4, pp. 359–369, 1994.

[7] A. Dogariu, A. Kuzmich, and L. J. Wang, "Transparent anomalous dispersion and superluminal light pulse propagation at a negative group velocity," *Phys. Rev. A*, vol. 63, pp. 053806-1–053806-12, 2001.

[8] L. J. Wang, A. Kuzmich, and A. Dogariu, "Gain-assisted superluminal light propagation," *Nature*, vol. 406, pp. 277–279, Jul. 2000.

[9] J. F. Woodley and M. Mojahedi, "Negative group velocity and group delay in left-handed media," *Phys. Rev. E, Stat. Phys. Plasmas Fluids Relat. Interdiscip. Top.*, vol. 70, no. 4, pp. 046603-1–046603-6, 2004.

[10] A. Dogariu, A. Kuzmich, H. Cao, and L. J. Wang, "Superluminal light pulse propagation via rephasing in a transparent anomalously dispersive medium," *Opt. Exp.*, vol. 8, no. 6, pp. 344–350, Mar. 2001.

[11] H. Cao, A. Dogariu, and L. J. Wang, "Negative group delay and pulse compression in superluminal pulse propagation," *IEEE J. Sel. Topics Quantum Electron.*, vol. 9, no. 1, pp. 52–58, Jan. 2003.

[12] R. Y. Chiao, "Faster-than-light propagations, negative group delays, and their applications," in *Proc. 22nd Phys. Commun. Solvay Conf. Phys.*, Nov. 2001, pp. 287–314, doi: 10.1142/9789812704634_0016.

[13] M. Kitano, T. Nakanishi, and K. Sugiyama, "Negative group delay and superluminal propagation: An electronic circuit approach," *IEEE J. Sel. Topics Quantum Electron.*, vol. 9, no. 1, pp. 43–51, Jan./Feb. 2003.

[14] T. Nakanishi, K. Sugiyama, and M. Kitano, "Demonstration of negative group delays in a simple electronic circuit," *Amer. J. Phys.*, vol. 70, no. 11, pp. 1117–1121, 2002.

[15] J. N. Munday and R. H. Henderson, "Superluminal time advance of a complex audio signal," *Appl. Phys. Lett.*, vol. 85, no. 3, pp. 503–504, Jul. 2004.

[16] D. Solli, R. Y. Chiao, and J. M. Hickmann, "Superluminal effects and negative delays in electronics, and their applications," *Phys. Rev. E, Stat. Phys. Plasmas Fluids Relat. Interdiscip. Top.*, vol. 66, no. 5, pp. 056601-1–056601-4, Nov. 2002.

[17] C. D. Broomfield and J. K. A. Everard, "Broadband negative group delay networks for compensation of oscillators using feedforward amplifiers," *Electron. Lett.*, vol. 36, no. 23, pp. 1710–1711, Sep. 2000.

[18] B. Ravelo, "X-band negative group-delay lossy stub line," *IET Microw., Antennas Propag.*, vol. 12, no. 1, pp. 137–143, 2018.

[19] G. V. Eleftheriades, O. Siddiqui, and A. K. Iyer, "Transmission line models for negative refractive index media and associated implementations without excess resonators," *IEEE Microw. Wireless Compon. Lett.*, vol. 13, no. 2, pp. 51–53, Feb. 2003.

[20] O. F. Siddiqui, M. Mojahedi, and G. V. Eleftheriades, "Periodically loaded transmission line with effective negative refractive index and negative group velocity," *IEEE Trans. Antennas Propag.*, vol. 51, no. 10, pp. 2619–2625, Oct. 2003.

[21] O. F. Siddiqui, S. J. Erickson, G. V. Eleftheriades, and M. Mojahedi, "Time-domain measurement of negative group delay in negative-refractive-index transmission-line metamaterials," *IEEE Trans. Microw. Theory Techn.*, vol. 52, no. 5, pp. 1449–1454, May 2004.

[22] G. Chaudhary and Y. Jeong, "Tunable center frequency negative group delay filter using coupling matrix approach," *IEEE Microw. Wireless Compon. Lett.*, vol. 27, no. 1, pp. 37–39, Jan. 2017.

[23] G. Liu and J. Xu, "Compact transmission-type negative group delay circuit with low attenuation," *Electron. Lett.*, vol. 53, no. 7, pp. 476–478, Mar. 2017.

[24] T. Shao, Z. Wang, S. Fang, H. Liu, and S. Fu, "A compact transmission-line self-matched negative group delay microwave circuit," *IEEE Access*, vol. 5. pp. 22836–22843, Oct. 2017.

[25] K. P. Ahn, R. Ishikawa, and K. Honjo, "Low noise group delay equalization technique for UWB InGaP/GaAs HBT LNA," *IEEE Microw. Wireless Compon. Lett.*, vol. 20, no. 7, pp. 405–407, Jul. 2010.

[26] K.-P. Ahn, R. Ishikawa, and K. Honjo, "Group delay equalized UWB InGaP/GaAs HBT MMIC amplifier using negative group delay circuits," *IEEE Trans. Microw. Theory Techn.*, vol. 57, no. 9, pp. 2139–2147, Sep. 2009.

[27] B. Ravelo, "Étude des circuits analogiques-numériques NGD et leurs applications: Théorie fondamentale et expérimentations des circuits analogiques et numériques à temps négatif et leurs applications," (in French), Éditions Univ. Européennes, PAR GmbH & Co. KG, Sarrebruck, Germany, Tech. Rep. 10802, Jan. 2012, ch. 10, p. 432.

[28] B. Ravelo, *Theory and Design of Analogue and Numerical Elementary NGD Circuits: Theoretical Characterization of Analogue and Numerical NGD Circuits*, Saarbrücken, Germany: LAP, Mar. 2012, p. 352.

[29] B. Ravelo, "Theory of coupled line coupler-based negative group delay microwave circuit," *IEEE Trans. Microw. Theory Techn.*, vol. 64, no. 11, pp. 3604–3611, Nov. 2016.

[30] B. Ravelo, "Similitude between the NGD function and filter gain behaviours," *Int. J. Circuit Theory Appl.*, vol. 42, no. 10, pp. 1016–1032, Oct. 2014.

[31] C.-T. M. Wu and T. Itoh, "Maximally flat negative group delay circuit: A microwave transversal filter approach," *IEEE Trans. Microw. Theory Techn.*, vol. 62, no. 6, pp. 1330–1342, Jun. 2014.

[32] M. Kandic and G. E. Bridges, "Asymptotic limits of negative group delay in active resonator-based distributed circuits," *IEEE Trans. Circuits Syst. I, Reg. Papers*, vol. 58, no. 8, pp. 1727–1735, Aug. 2011.

[33] G. Chaudhary and Y. Jeong, "A finite unloaded quality-factor resonators based negative group delay circuit and its application to design power divider," *Microw. Opt. Technol. Lett.*, vol. 58, no. 12, pp. 2918–2921, Dec. 2016.

[34] B. Ravelo, "Baseband NGD circuit with RF amplifier," *Electron. Lett.*, vol. 47, no. 13, pp. 752–754, Jun. 2011.

[35] B. Ravelo, "Synthesis of RF circuits with negative time delay by using LNA," *Adv. Electromagn.*, vol. 2, no. 1, pp. 44–54, Feb. 2013.

FAYU WAN (M'18) received the Ph.D. degree in electronic engineering from the University of Rouen, Rouen, France, in 2011. From 2011 to 2013, he was a Post-Doctoral Fellow with the Electromagnetic Compatibility Laboratory, Missouri University of Science and Technology, Rolla. He is currently a Full Professor with the Nanjing University of Information Science and Technology, Nanjing, China. His current research interests include negative group delay circuits, electrostatic discharge, electro-magnetic compatibility, and advanced RF measurement.

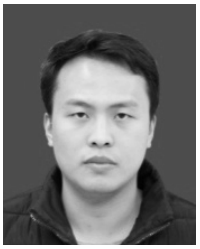

NINGDONG LI received the B.Sc. degree in electrical engineering from Anhui Polytechnic University, Wuhu, China, in 2017. He is currently pursuing the M.S. degree from the Nanjing University of Information Science and Technology, Nanjing, China. His research interests include abnormal-wave propagation in dispersive media and microwave circuits.

BLAISE RAVELO (M'08) received the Ph.D. degree from the University of Brest in 2008 and the dissertation led to research (HDR = Habilitation à Diriger des Recherches) from the University of Rouen in 2012.

He is currently an Associate Professor with the Graduate Engineering School, ESIGELEC, IRSEEM, Rouen, France. He is a pioneer of the negative group delay RF/analog and digital circuits, and systems. He has (co)-authored over 200 papers and is regularly involved in national/international research projects. He co-supervised and directed nine Ph.D. students and six Ph.D. candidates. He participates regularly in large research and development international projects. His research interests cover microwave circuit design, electromagnetic compatibility and interference, and signal and power integrity engineering. His current publication h-index is 16 (Reference: Google Scholar 2017).

Dr. Ravelo has been an URSI Member and regularly invited to review papers submitted to international journals (the IEEE TMTT, the IEEE Access, the IEEE TCS, the IEEE TEMC, the IEEE TIM, the IEEE TIE, the *Journal of Electromagnetic Waves and Applications*, the IET CDS, the IET MAP, the *International Journal of Electronics*, and so on) and international books (Wiley, Intech Science, and so on). He is a member of the Advanced Electromagnetic Symposium 2013–2018 Technical Committee and the IEEE RADIO 2015 Scientific Committee and the Scientific Chair of the 5th International Conference on Electromagnetic Near-Field Characterization and Imaging in 2011.

QIZHENG JI received the M.S. degree in aircraft design from the China Academy of Space Technology (CAST), Beijing, China, in 2006. He is currently a Senior Engineer in technology and management of electrostatic protection with the Beijing Orient Institute of Measurement and Test, CAST. His research interests include microwave circuits and ESD.

BINHONG LI received the M.S. degree in micro and nanoelectronics from the University of Grenoble, France, in 2008, and the Ph.D. degree in EMC and reliability of ICs from the Institut National des Sciences Appliquées, Toulouse, France, in 2011. He joined the Institute of Microelectronics, Chinese Academy of Sciences, Beijing, China, in 2012, where he is currently an Associate Professor in SOI circuit and device reliability and EMC.

JUNXIANG GE received the Ph.D. degree in radio engineering from Southeast University, Nanjing, China, in 1991. He has been the Dean of the School of Electronic and Information Engineering, Nanjing University of Information Science and Technology, Nanjing, since 2011. His current research interests include electromagnetic field theory, microwave and millimeter-wave technology, and antenna.